Nigerian Research Journal of Engineering and Environmental Sciences 9(2) 2024 pp. 848-863
p ISSN: 2635-3342; e ISSN: 2635-3350

Nigerian Research Journal of Engineering and Environmental Sciences
Journal homepage: www.rjees.com

Original Research Article

Carbonated Sandcrete-Nanographene Oxide Mortar: Investigating Morphology, Phase Formation, and CO_2 Sequestration for Enhance Durability

***[1]Abdullahi, M., [2]Odigure, J.O., [3]Yabagi, I.A. and [4]Azeez, S.O.**

*[1]Department of Chemical Engineering, The Federal Polytechnic, P. M. B 55, Bida, Nigeria.
[2]Department of Chemical Engineering, Federal University of Technology, Minna, Nigeria.
[3]Department of Civil Engineering, The Federal Polytechnic, P. M. B 55, Bida, Nigeria.
[4]Department of Chemistry and Industrial Chemistry, Faculty of Pure and Applied Sciences, Kwara State University, Malete, Nigeria.
*tsowagba@yahoo.com

http://doi.org/10.5281/zenodo.5045452

ARTICLE INFORMATION

Article history:
Received 14 Nov. 2024
Revised 06 Dec. 2024
Accepted 07 Dec. 2024
Available online 30 Dec. 2024

Keywords:
Sandcrete-nGO
CO_2 sequestration
Morphology
Carbonation
Hydration
Durability

ABSTRACT

The escalating trend in carbon dioxide emissions is unequivocally linked to global warming and climate change phenomena. This study investigated the morphological development and phase formation of carbonated sandcrete-nanographene oxide (S-nGO) composite mortar for CO_2 sequestration and durability under ambient conditions (30±2 °C; 50% RH) after 28 days. A comprehensive characterization methodology incorporating X-ray Diffractometer (XRD), X-ray Fluorescence (XRF), Thermogravimetry Analysis (TGA), Fourier Transform infrared Spectroscopy (FTIR), Energy-Dispersed Spectroscopy (EDS), and Scanning Electron Microscopy (SEM) was used to establish correlations between microstructural changes, degree of porosity, CO_2 sequestration, and carbonate concentration. Incorporating nGO during the carbonation transformation in cement-based composites substantially alters the sandcrete matrix's hydration kinetics and associated hydrates, exerting a profound influence on the hydration mechanism. Unlike the control without nanographene oxide, the SEM of S-nGO matrix composites showed a dense microstructure characterized by a foil-like morphology of calcium silicate hydrate (C-S-H) phase containing more carbon, calcium, oxygen, and silicon. The 0.05% S-nGO composite mixture resulted in the highest carbon dioxide sequestration potential, with a carbonate concentration of 0.0406 kg/m^3, whereas that of the 0% nanographene oxide control sample was approximately 0.0128 kg/m^3 at 30 °C. The findings demonstrated that early-age carbonation (1–28 days) could enhance the durability of the sandcrete–nanographene oxide composite by refining the microstructure and reducing the porosity, thereby improving the material's overall properties and carbon sequestration potential.

1. INTRODUCTION

The pervasive utilization of sandcrete materials in infrastructure development throughout Nigeria and Africa has underscored their importance in the contemporary building industry. Nevertheless, the durability of sandcrete is significantly impacted by carbonation, highlighting the need for a

comprehensive understanding of the microstructure of sandcrete and its effects on longevity (Abdullahi *et al.,* 2016). Research into the microstructural characteristics of sandcrete remains a paramount focus area, driving efforts to optimize the performance and service life of sandcrete materials in various applications. The key traditional material in sandcrete production is cement which has a destructive effect on the environment. Research is ongoing in multiple fields to replace cement-based materials with less clinker and improve the traditional reinforcement method (Jafarnia *et al.,* 2020; Abdullahi *et al.,* 2024; Fonseka *et al.,* 2024). The partial replacement of the traditional materials with nanographene oxide (nGO) could be the paradigm shift in building materials with improved physicochemical characteristics. Numerous studies have demonstrated that incorporating GO profoundly induces microstructural modification, resulting in improved densification and resistance to degradation (Liu *et al.*, 2021; Chu *et al.,* 2020; Fonseka *et al.,* 2024; Lin *et al.,* 2016; Yang *et al.,* 2017).

Sandcrete materials' microstructure can be investigated through electron, optical, and scanning probe microscopy. These analyses examine structural transformation, and elemental and mineral compositions, revealing the molecular vibrational mode and thermal transition, offering valuable insight into their structural and thermal behaviour (Cui *et al.,* 2017). Cement-based materials' performance is influenced by transport mechanisms influenced by a complex interplay of factors, encompassing characteristics such as pore volume fraction, pore size distribution, pore type, pore network connectivity, and arrangement of material crystals within the solid matrix. This intricate interplay determines the transport mechanism and kinetics, ultimately controlling the material durability and performance (Naik and Kumar, 2010; Handayani *et al.,* 2019). Lv *et al.* (2013) studied the morphological characteristics of hydrated cement-based composite reinforced with various percentages of GO using SEM. They observed acicular and columnar crystals for the control hydrated products without GO. However, a dense microstructure was observed for 0.01-0.03 wt% GO composite mix with a flower-like crystal. As the percentage of GO increased from 0.04-0.05 wt%, the hydration products steadily transform into regular polyhedron crystals with enhanced densification.

The carbonation process in cement-based materials is significantly influenced by pore saturation and porosity. Studies by Shah (2005), Varzina *et al.* (2022), and Naik *et al.* (2009) revealed that during carbonation, a decrease in porosity and moisture availability markedly influences the material diffusion coefficient and water penetrability, as CO_2 and other mineral ions ingress into the cement-based material, thereby affecting its susceptibility to carbonation. Rostami *et al.* (2012) study the microstructure of cement pastes during early-age carbonation curing, shedding light on the mechanisms governing concrete carbonation. Their study highlighted the benefits of early carbonation curing in achieving improved strength and enhanced material durability. Additionally, carbonation facilitates the formation of three polymorphic calcium carbonate variants via CO_2 diffusion, resulting in a microstructure characterized by densely packed, circular crystals (< 3 μm). The study by Devi and Khan (2020) demonstrated that increased GO concentration and curing time collectively contribute to reduced carbonation depth in concrete utilizing recycled aggregate. Long *et al.* (2018) utilized TGA to examine the carbonization kinetics of C-S-H gel, demonstrating that GO enhances stability during early carbonation. According to Lv *et al.* (2016), the depths of carbonation of GO-containing samples were notably lower, demonstrating reductions of 78.57 and 65.71% at 7 and 28 days, respectively, compared to the control samples. Mohammed *et al.* (2018) posit that GO restricts the diffusion of CO_2 molecules into cementitious materials by refining their microstructure and diminishing porosity.

Atmospheric carbon dioxide (CO_2) capture has been facilitated through the development of diverse methodologies and technologies (Sunho *et al.,* 2009; Gajda, 2001). Despite the existing challenges, sandcrete-based CO_2 sequestration emerges as a promising solution for curbing acidic emissions in developing countries. Most researchers cited utilizing co-citation mapping technique, nanographene oxide-induced sandcrete structural modification for CO_2 capture and its effect on sandcrete carbonation has not been thoroughly investigated A considerable knowledge gap exists. A comprehensive review of the literature reveals ambiguities and discrepancies in the role of GO in the microstructure characterization of hydrated cement composites. Addressing this area is pivotal in advancing current

scientific knowledge on sandcrete carbonation and its environmental impact as carbon dioxide concentration in the atmosphere rises**.** This study examines the microstructural changes and to quantify the degree of CO_2 sequestration in a sandcrete-nanographene oxide composite subjected to early-age atmospheric carbonation curing under ambient conditions.

2. MATERIALS AND METHODS

2.1. Material Collection and Preparation of Samples

An outcome-based method for the determination of carbonated microstructure development of 0, 0.01, and 0.050% S-nGO composites was carried out. The microstructural characteristics of the composite mixtures were compared to standard sandcrete (NIS, 2007). A standard Portland cement (Dangote Cement) meeting ISO 9001:2008 certification and sharp sand conforming to the American Standard (ASTM C33) were utilized for the study. Figure 1 displays the particle size distribution of the sand aggregate. The sand has a density of 2660 kg/m^3 with 0.92% minimal moisture concentration, and a uniformity coefficient of 2.95. The nanographene oxide used for the study was obtained from Sigma Aldrich Chemie Company, UK, while the potable water satisfies NIS 554: 2007 and was used in the preparation of the sample mortar. The research utilized advanced materials characterization instrumentation, comprising: X-ray Diffractometer (XRD) utilizing DY614 Empyrean by Panalytical; Energy Dispersive X-ray Fluorescence (EDXRF) analysis using MiniPal4 embedded with X'pert HighScore Plus Software; High-resolution imaging and microanalysis through Scanning Electron Microscopy (SEM) with Field Emission Gun Nova NanoSEM 230; Elemental composition analysis using Elemental Diffraction Spectrometer (EDS) Oxford X-Max Detector, operated with INCA Software to characterize the starting materials to ascertain the oxide proportions, mineralogical properties, microstructural evolution and elemental compositions, respectively.

2.2. Sandcrete Mortar Production

Two distinct mortar samples, labelled Q and R, were prepared with consistent workability per set. Q serves as the reference comprised of five (5) samples (Q1– Q5) prepared by standard mix design specification based on NIS specification (2007). In contrast to set Q, set R had varying proportions of nGO replacing the sand. Set R is delineated into two distinct subsets, labelled $R_{0.01\text{-}R1} – R_{0.01\text{-}R5}$ and $R_{0.05\text{-}R1} – R_{0.05\text{-}R5}$. Each subset consists of 5 samples partially replacing sand with 0.01 and 0.050% nanographene oxide. The design mix proportion for samples Q and R, are presented in Table 1. A consistent cement-to-sand ratio of 1:6 (Anosike and Oyebade, 2012; NIS, 2007; Omoregie, 2012) and water-to-cement ratio (W/C) of 0.5 (Omoregie, 2012; Anosike and Oyebade, 2012; NIS, 2007) were used in the study.

Table 1: Mixed proportions of standard mortar (reference) and sandcrete-nanographene oxide (S-nGO)

Mix design	Q_1-Q_5	$R_{0.01\text{-}R1}$- $R_{0.01\text{-}R5}$	$R_{0.05\text{-}R1}$- $R_{0.05\text{-}R5}$
Temperature (ºC)	30±2	30±2	30±2
% Replacement	-	0.01	0.05
Cement (g)	33.71	33.71	33.71
Sand (g)	202.29	202.088	201.279
nGO (g)	-	0.2023	1.0115
Water (g)	16.85	16.85	16.85
Curing age (day)	1- 28	1- 28	1-28
Water/cement	0.5	0.5	0.5

All the mortar samples were prepared in the laboratory based on Abdullahi *et al.* (2016) and NIS (2007). The nGO sheets were added to the mixture at 0% (control), 0.01%, and 0.05% by weight of the sand. A 10-minute ultrasonic mixing process was performed with 16.85 g of water added to facilitate a thorough and homogeneous dispersion of the nGO, resulting in a uniform nanocomposite mixture. The

freshly mixed sandcrete was rammed into a pre-oiled mould and compacted via a standard tapping bar. The cast samples were detached from their moulds after 24 hours and subjected to a 1–28-day curing process under laboratory conditions (30±2 °C, 50% RH) to facilitate hydration and strength development. After 24 hours of curing under ambient conditions, a sample (Q1, $R_{0.01\text{-}R1,}$ and $R_{0.05\text{-}R1}$) was removed and crushed via a hydraulic-powered Press Machine Model: Cl-03 DYE-2000 Wuxi OKE Electronic Co., Ltd., Fujita, Japan, at a 0.05 kN/s loading ratio. Moreover, porosity tests were carried out based on differences in mass, as depicted in Equation 1, following ASTM C1585/C1585M-13 (2019) and Odeyemi *et al.* (2018).

$$\text{Porosity (\%)} = (W_{s2} - W_{s1})/W_{s1} \quad (1)$$

where W_{s1} is the initial mass of the dry sandcrete sample (g) and W_{s2} is the final mass of the wet sandcrete sample (g).

The crushed samples were further pulverized and subjected to advanced analysis via XRD, SEM, EDS, XRF, FTIR, and TGA/DTA to characterize the mineral components, microstructural changes, elemental and oxide compositions, bonding structure, and degree of carbonate formation, respectively. The same technique was adopted for samples Q_2 - Q_5, $R_{0.01\text{-}R2}$ - $R_{0.01\text{-}R5}$, and $R_{0.05\text{-}R2}$ - $R_{0.05\text{-}R5}$.

3. RESULTS AND DISCUSSION

3.1. Composite Grading

Figure 1 illustrates the size distribution curves for sand and sand–nanographene oxide (S-nGO) composites used to produce the cubic samples. The granulometric analysis revealed that the silt content was low (less than 5%), thereby increasing the workability, minimizing particle segregation and bleeding, and enhancing the compactness of the sandcrete mortar (Raina and Goyal, 2015).

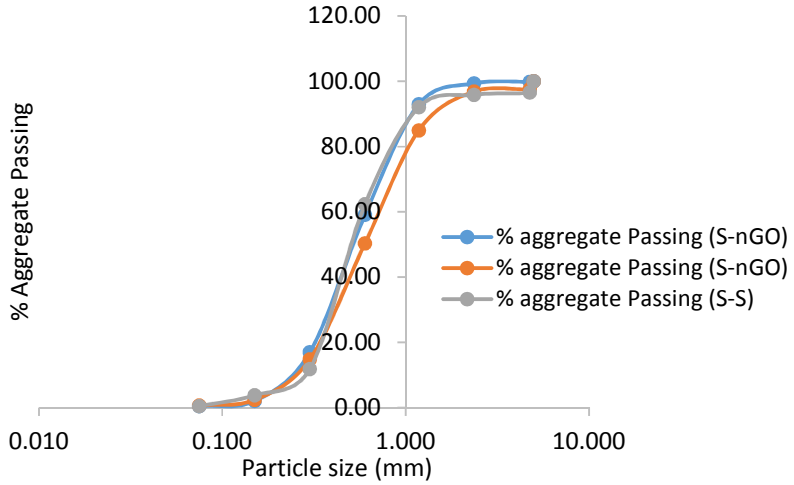

Figure 1: Sieve analysis of the S-S and S-nGO composites

3.2. Chemical Composition, Mineralogical Properties, and Morphological Evaluation of Starting Materials

The study characterizes the composition and microstructure of a composite mixture consisting of sand, nanographene oxide (nGO), and cement as depicted in Table 2 and Figures 2 to 6. The oxide analysis in Table 2 reveals the cement is primarily composed of CaO (69.01%) and SiO_2 (17.897%), adhering to ASTM C150 specifications. The sand and nGO exhibit distinct compositions, with silica dominating the former (89.029%) and trace metallic oxides present in the latter as shown in Table 2. Nitrogen BET adsorption measurements indicate high specific surface area for cement (83.613 m^2/g) and nGO (148.403 m^2/g), facilitating rapid hydration and densification. Figure 2 showed the elemental spectra

analysis of the starting materials. The result depicts the presence of major amount of calcium, silicon, oxygen and carbon which substantiate the findings in Table 2. The Scanning electron microscopy (SEM) shown in Figures 3-5 confirms uniform particle distribution of the starting materials, while X-ray diffraction (XRD) analysis in Figure 6 identifies silica, graphite, gypsum, and muscovite in the samples. These findings align with existing literature (Abdullahi *et al.,* 2010; Song *et al.,* 2014) providing valuable insight into the composite's properties.

Table 2: Comparative XRF analysis of sand, cement, and nanographene oxide

Oxide	Cement (%)	Sand (%)	nGO (%)
Fe_2O_3	1.151	0.4016	0.15172
CuO	0.01038	0.04519	0.00704
ZnO	0.00332	0.00705	0.00378
MgO	2.65	2.39	0.00
Al_2O_3	5.531	8.415	0.309
SiO_2	17.897	89.029	0.2856
P_2O_5	0.1055	0.336	0.0912
SO_3	3.5227	0.0435	0.3073
Cl	0.0283	0.0047	0.01516
K_2O	0.5049	0.1347	0.1343
CaO	69.01	0.129	0.4592
TiO_2	0.0777	0.301	0.01015

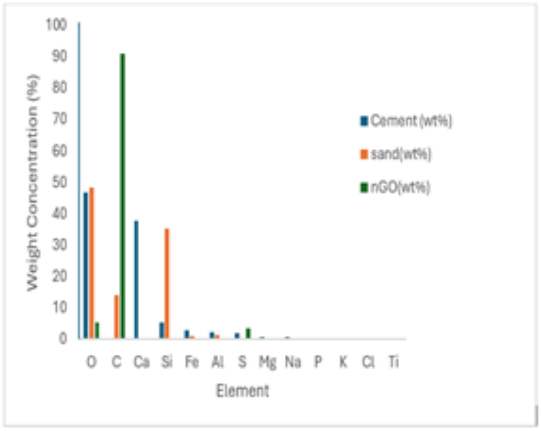

Figure 2: EDS analysis of sand, cement and nGO

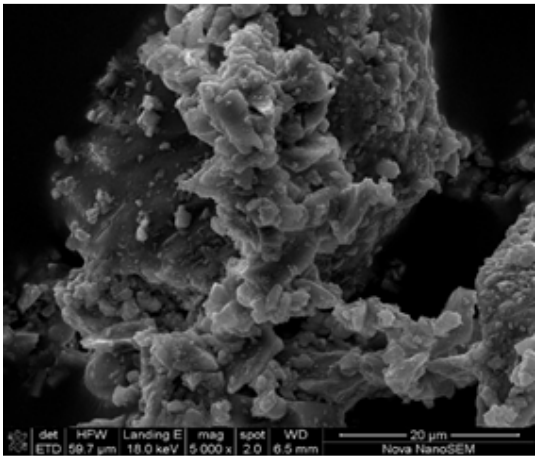

Figure 3: SEM photomicrograph of cement

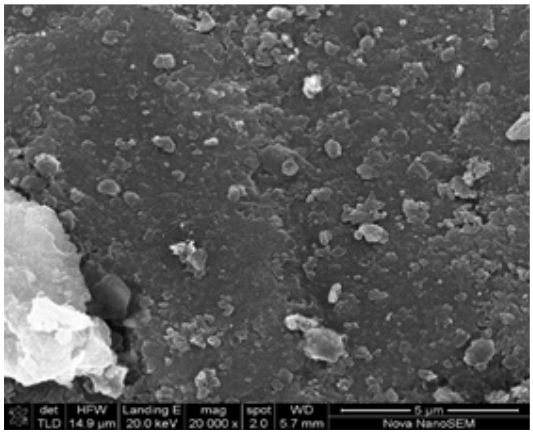

Figure 4: SEM image of the sand

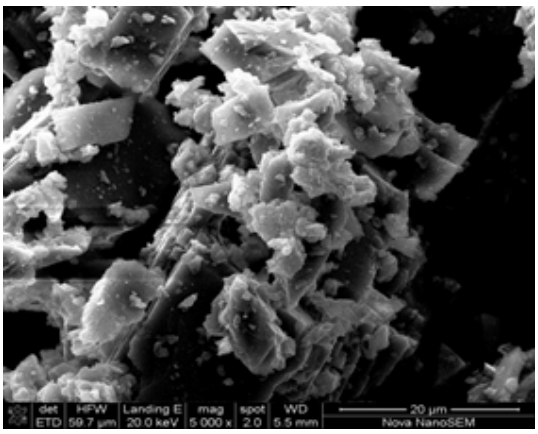

Figure 5: SEM image of the nano-graphene oxide

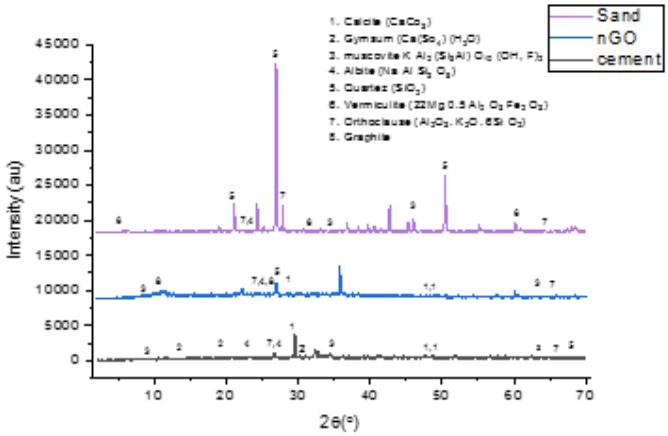

Figure 6: Comparative XRD analysis of all the sandcrete constituents

3.3. Water Content

The ratio of water to cement in conjunction with nGO produced a paste with a suitable optimal consistency and sufficient workability because of its high specific surface area coupled with its strong affinity to absorbed water (Fernandez *et al.,* 2004; Odigure, 1996). This characteristic plays a substantial role in contributing hydroxyl groups (OH^-) to the hydration reaction products. The improved dissolution of nGO in the hydrated cement-based matrix could be attributed to the removal of the -C-O-C- group on nGO minimizing the interaction complexation between Ca^{2+} and nGO. This facilitates water interaction reaction with cement and other minerals inducing the nucleation and growth of calcium-silicate-hydrate (C-S-H) gel. The gel in turn reacts with nGO to form strong interfacial bonds, resulting in improved mechanical and durability properties, as shown in Equation (2), and a covalent bonding structure. Sandcrete is a highly porous cement-based composite with intrinsic weakness, leading to crack development, and is prone to dead loading and degradation. The addition of nGO to the sandcrete composite as the hydration reaction progresses with time results in a refined microstructure with flower-like crystals of the nGO-C-S-H gel, which gradually densifies the composite matrix as the percentage of nGO increases from 0.01 to 0.05%, as depicted in Figures 7 and 8. Conversely, the control sample (S□S) displayed a needle-like C-S-H gel stacked haphazardly in the composite matrix with increased micropores, as shown in Figure 9.

$$\text{nGO-OH} + \text{Si-OH (C-S-H)} \rightarrow \text{Si-O-nGO} + H_2O \quad (2)$$

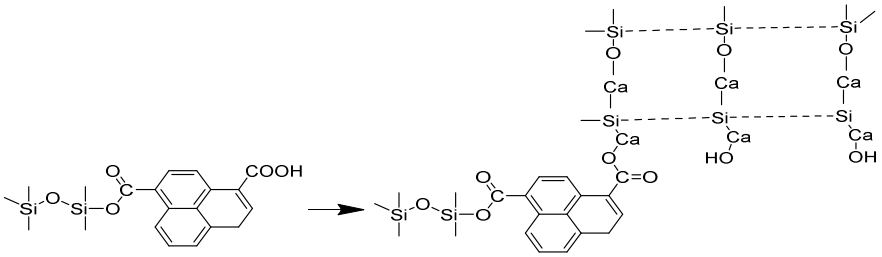

SiO_2 nGO SiO_2-nGO-C-S-H

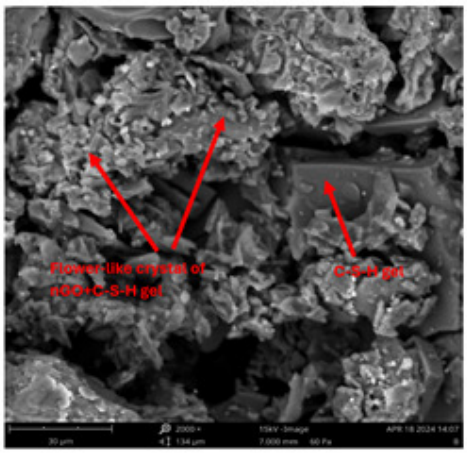

Figure 7: Dense microstructure of 0.01% S-nGO composite after 28 days of curing

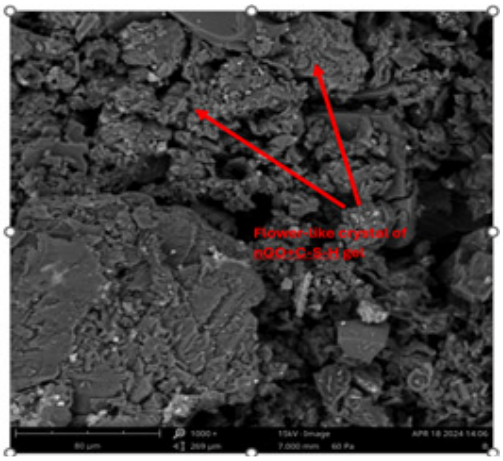

Figure 8: Denser microstructure of 0.05% S-nGO composite after 28 days of curing

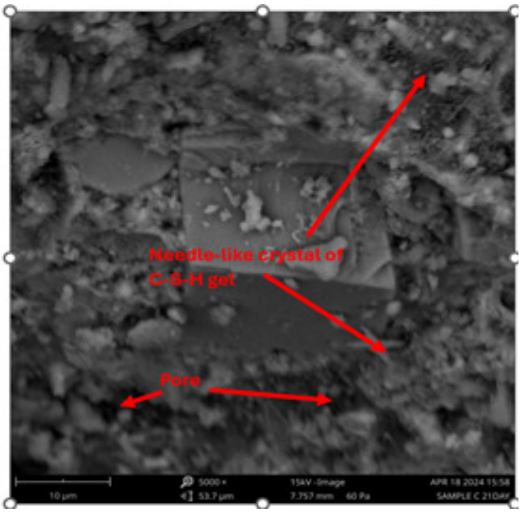

Figure 9: S□S microstructure after 28 days

3.4. Performance characteristics: Porosity and CO_2 sequestration

Figure 10 shows the porosities of the 0, 0.01, and 0.050% sandcrete-nanographene oxide (S-nGO) composites and control samples (standard sandcrete) as a function of age at 30±2 °C for 1, 7, 14, 21 and 28 days, respectively. Generally, the experimental data did not diverge from the expected pattern under constant thermal conditions. That is, as CO_2 is taken into the sandcrete composite, the porosity reduces with increasing carbonation with age. The porosity and granulometric size of mixed materials have

significant influence on the reaction rate by controlling water and CO_2 accessibility into the composite matrix to the unreacted core interface ((Fernandez *et al.,* 2004; Odigure, 1994; Younsi *et al.,* 2013). As proven by the kinetic behaviour, as it affects the porosity, the instantaneous porosities of the S-nGO and control composite samples are initially high, attributed to low concentration of calcium and silicon ions in the sandcrete pore solution (Abdullahi *et al.,* 2016). With increasing concentration of cations as CO_2 dissolves in the pore solution, the porosity decreases sharply after 28 days attributed to carbonate deposition within microporous framework and the intercalation reaction.

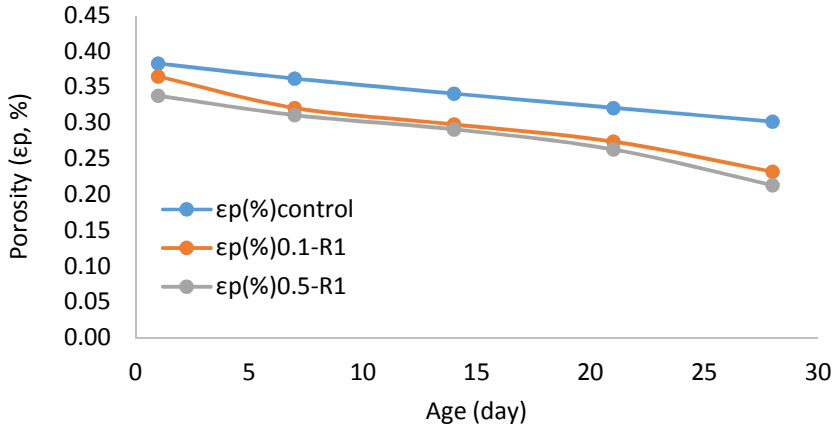

Figure 10: Porosity of 0.010, 0.050% S-nGO and S-S (control) under ambient conditions

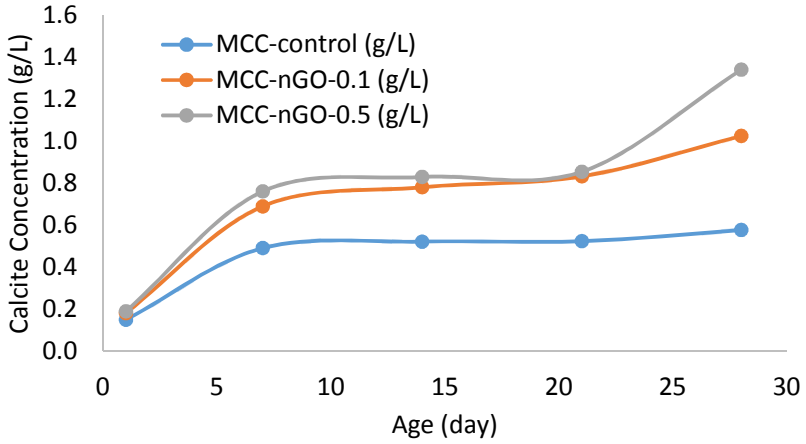

Figure 11: Carbonate concentrations for 0.01, 0.050% S-nGO and S-S composites under ambient conditions

Quantitatively, for the 0.010% S-nGO composite, the porosity decreases from 0.365–0.232 (36.4%) after 28 days of carbonation under ambient conditions. The same patterns were observed for the 0.050% S-nGO (0.338 - 0.213) (37%) composites under ambient conditions, whereas the porosity of the control samples decreased by 21.2% for the same curing age. The decrease in porosity could be attributed to convoluted carbonation reactions occurring as CO_2 is taken into the composite matrix coupled with the interaction of nanographene oxide and cement hydrated gel (C-S-H) in the micropores, as depicted in Figure 11 and corroborated by the SEM micrographs shown in Figures 12 and 13 respectively. The absence of nGO in the control sample resulted in high porosity and low carbonate concentration, as depicted in Figures 11 and 14. The densification of the S-nGO composites, irrespective of the percentage of nanographene oxide in the mixture, could be due to direct carbonation of the dissolved cement hydrated products (portlandite and binding gels) with carbon dioxide and the homogeneous distribution of nGO in the composite matrix, as shown in Equations (3-5).

$$Ca(OH)_2 + H_2CO_3 \rightarrow CaCO_3 + 2H_2O \quad (3)$$

$$3CaO.2SiO_2.3H_2O + 3CO_2 \rightarrow 3CaCO_3 + 2SiO_2 + 3H_2O \quad (4)$$

$$4CaO{\cdot}Al2O3{\cdot}13H2O + 4CO_2 \rightarrow 4CaCO_3 + 2Al(OH)_3 + 10H_2O \quad (5)$$

The mixture of nGO and C-S-H gel that bind the sandcrete particles together improves the durability of the nGO-sandcrete composites, as the oxygen group binds the products together, especially to Ca^{2+} (intercalation). In addition, the excess Ca^{2+} from C-S-H gel and $Ca(OH)_2$ in the pore fluid reacts with carbonic acid to produce calcite. This phenomenon tends to enhance the density and minimized the micropores in specimens $R_{0.01}$ and $R_{0.05}$ compared with those of the control samples. This is evident in the photomicrographs shown in Figures 12–14 respectively.

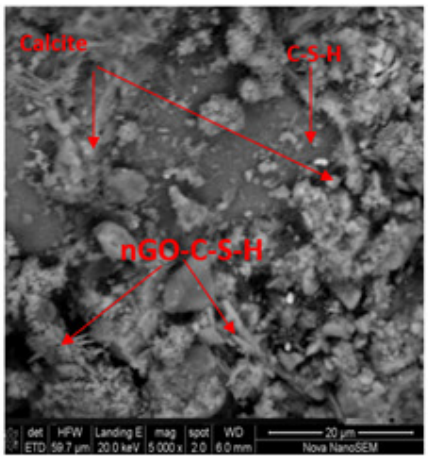

Figure 12: SEM image of 0.010% S-nGO after 28-day of carbonation

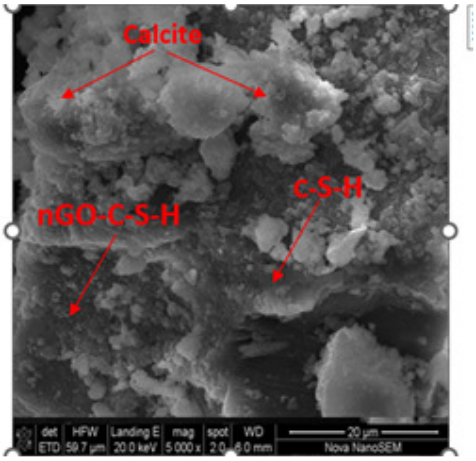

Figure 13: SEM image of 0.05% S-nGO at after 28-day of carbonation

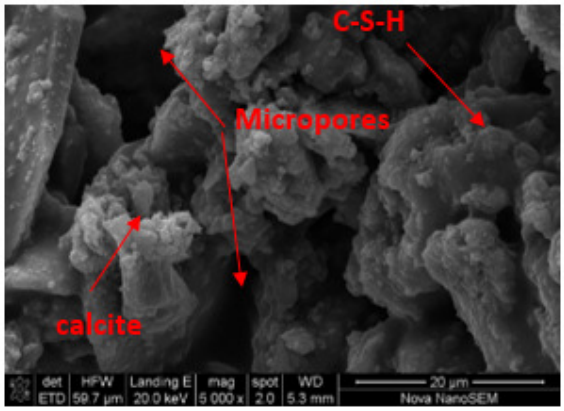

Figure 14: SEM image of S-S (control) after 28-day of carbonation

The processes of carbon sequestration through carbonation for the 0.010% and 0.050% S-nGO composites and the control sample at various ages are presented in Figure 11. Generally, the results revealed an increase in carbonate concentration with age as CO_2 was transformed into stable carbonates. The results presented in Figure 11 for 0.010% and 0.050% S-nGO presented increased carbonate concentrations, which ranged from 0.183-1.026 g/L (82.2%) and 0.191-1.342 g/L (85.8%), respectively, after a 28-day carbonation period. The control sample (Figure 11) also showed the same trend under the same experimental conditions, with carbonate concentrations ranging from 0.151- 0.578 g/L. This increase could be linked to the increased ionic activity, high early-age porosity, and favourable temperature regime. These factors promote accelerated nucleation and growth of metallic carbonates

($CaCO_3$) crystal. Researchers (Arya and Seena, 2024; Wang *et al.,* 2015) have reported that in the presence of reactive silica, portlandite reacts to yield diverse calcium-silicate-hydrate solid solutions. The increased carbonate concentration for the reference sample (Figure 11) is attributed to the carbonation of the cement hydrated gels (C-S-H and C-A-H) and portlandite produced as cement hydrate in the sandcrete matrix. However, the carbonate concentration of the control sample was lower than those of the 0.010 and 0.050% S-nGO composites subjected to the same conditions. This might be due to inadequate metallic ions and the gradual release of calcium and carbonate ions as cement hydrates. This is consistent with the results from the SEM micrographs (Figures 12 - 14) and porosity values obtained experimentally. The chemical reaction involving hydrated cement gels with dissolved CO_2 to form stable calcium carbonate (calcite) is enhanced by the comminution of nanographene oxide, which exposes the hydrophilic sites on the edge of the nanographene oxide lamellae (Lima-de-Farie, 1994). The nGO sheet attached to the binding gel (C-S-H) forms a 3-dimensional network, thereby creating a dense microstructure with increased strength. Studies have shown that the characteristic properties of nanographene oxide strongly depend on the exposed atoms (Lima-de-Farie, 1994). The micrographs of the 0.010% and 0.050% S-nGO composites under ambient conditions after 28 days of carbonation revealed increased densification of the morphology as more carbonates precipitated in the matrix. The micrographs, however, did not show a direct relationship with humidity or the ingress of oxygen. These factors are not reflected in the current study. The results revealed a foil-like C-S-H morphology and carbonate crystals closely intergrown within the solid phases. SEM micrographs revealed that nGO has a profound impact on the microstructure of the hydrated cement phase, as it interacts with the C-S-H gel precipitate with stable interfacial bonds, significantly increasing the toughness and durability and minimizing the brittleness of the sand-concrete composite. Compared with those with 0.01% nGO and the control, the samples with 0.05% nGO showed greater densification with reduced porosity after 28 days of curing.

3.5. EDS Characterization

The EDS analysis for the 0.010%, 0.050% S-nGO composites and the reference sample at 30±2 °C are presented in Figure 15. This finding corroborates previous observations of enhanced carbonate precipitation in S-nGO composites displaying high carbon (C), calcium (Ca), and oxygen (O) intensities. The high concentration of designated elements (C, Ca and O) suggests the presence of dissociating $CaCO_3$ after a 28-day period. EDS analysis showed no detectable carbon (C) in the reference sample. This phenomenon could be associated with slow carbonation reaction rate as CO_2 ingresses into the sandcrete matrix exhibiting high porosity when compared to S-nGO composites. The high oxygen intensity for the reference and S-nGO hydrated samples indicate the presence of portlandite and -OH groups generated as cement hydrates in the microporous matrix.

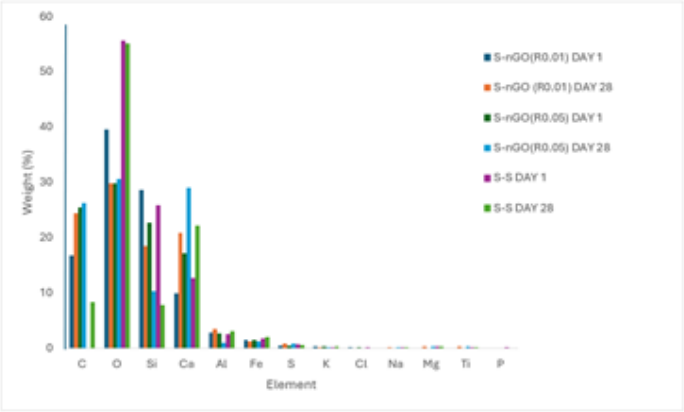

Figure 15: EDS characterization of control (S-S), 0.01% and 0.050% S-nGO composite under ambient conditions

3.6. Crystallographic Analysis

Figures 16-18 showed the XRD spectra patterns of the 0.01 and 0.050% S-nGO composites and the control sample under ambient conditions. A comparison of the XRD patterns of the 0, 0.01, and 0.05% S-nGO composites in Figures 16-18 indicates that the portlandite proportions are significantly reduced after 28 days of carbonation, whereas calcite is generated at the same time. Noticeable increases in the calcite peak intensities were observed for the S-nGO composite, whereas for the control sample, a high peak intensity for portlandite was observed. Hence, the S-nGO composites showed significant carbonation with increased carbon dioxide sequestration, as shown in Figures 16 and 17, compared with Figure 18 for the control sample.

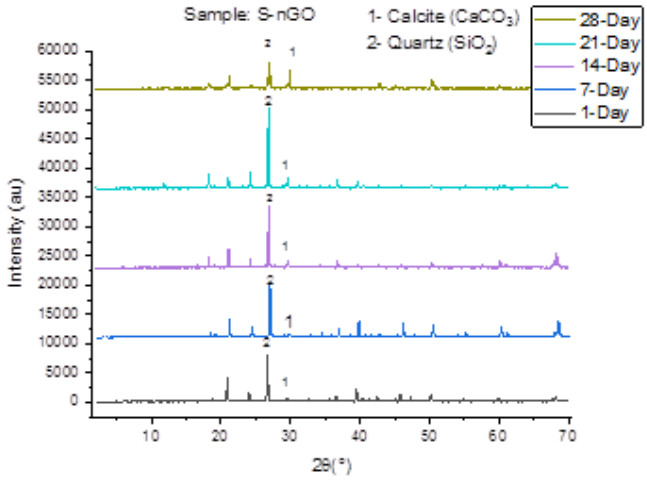

Figure 16: Comparative XRD analysis of the 0.01% S-nGO matrix composite

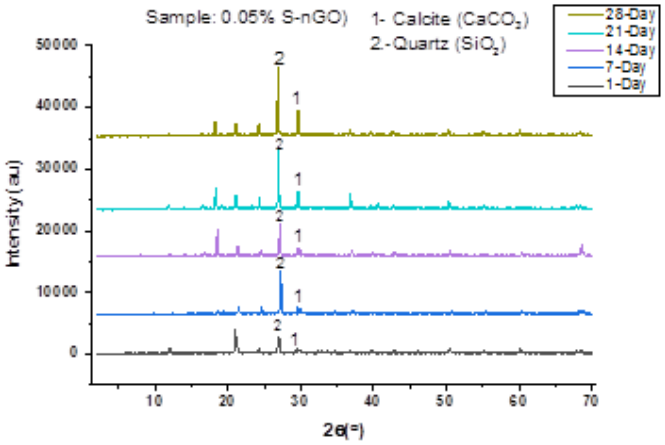

Figure 17: Comparative XRD analysis of the 0.050% S-nGO matrix composite for 1--28 days

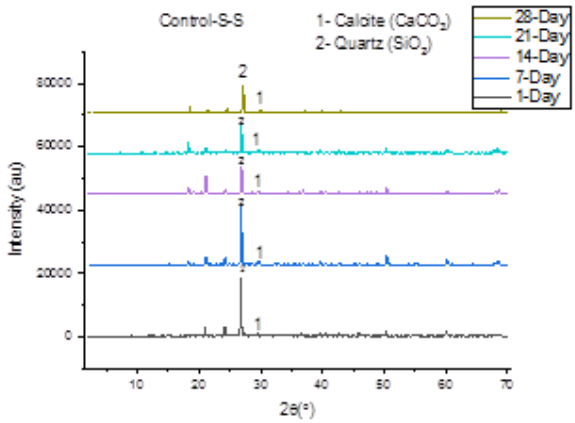

Figure 18: Comparative XRD analysis of standard sandcrete (control) for 1–28 days

3.7. TGA Analysis

The calcite formed for the S-S and S-nGO composites after 1 and 28 days is evident in the TGA analysis shown in Figure 19. The results revealed samples degradation in terms of percentage weight loss as the temperature increased from 30 – 950 °C. At 100–300 °C, the moisture present in the sample spores, the walls of the spores, and the surface of the nGO sheets (-OH) is lost (Chang and Chen, 2006). Between 500 and 950 °C, the weight loss is attributed to the thermal decomposition of calcite and the breaking of carbon-oxygen bonds, resulting in the removal of the hydroxyl group, as shown in Equations (6) and (7). Equation (7) represents the removal of (-OH) from the surface of the simplified hydrated cementitious nGO to reduce nGO and water vapour. The dehydroxylation of portlandite and C-S-H gel could be responsible for the high percentage of weight loss for the S-S and S-nGO samples after 1 day (Singh *et al.,* 2015).

$$CaCO_3\,(s) \rightarrow CaO\,(s) + CO_2\,(g) \quad (6)$$

$$C_6O_2(OH)_2(COOH)_{0.5}(O)_{0.5} \rightarrow C_6O\,(rGO) + H_2O\,(\text{water vapour}) \quad (7)$$

This is corroborated by the dense microstructure of calcite shown in the SEM micrographs in Figures 12 and 13.

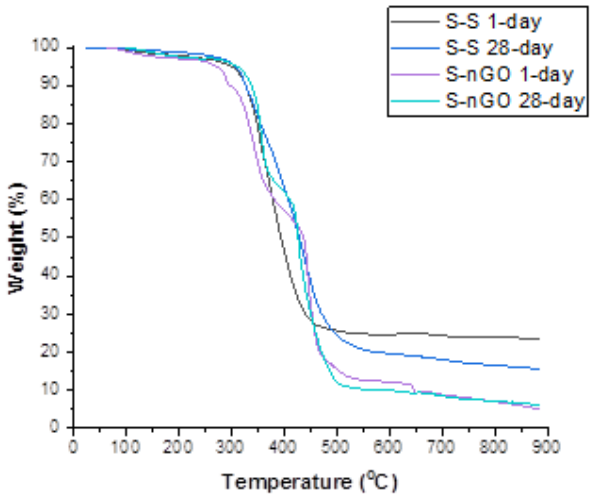

Figure 19: TGA analysis of the S-S and S-nGO composites for 1–28 days

3.8. FTIR analysis

Figure 20 presents the FT-IR analysis of the sandcrete composites (S-S, and S-nGO) after 1- and 28-day curing under ambient conditions, revealing the calcite ($CaCO_3$) formation due to carbon dioxide ingress into the composite matrix. The spectra revealed intense bands between 500 and 1550 cm^{-1}, indicating significant molecular interactions and vibrational resonances. The spectral peak at 1500 cm^{-1} is associated with sandcrete carbonation and is indicative of cross-linking reactions (SiO_2-nGO-C-S-H) and network formation within the composite materials. A significant increase in peak intensity was observed in the S-nGO composite at this band after 28 days, indicative of enhanced calcite formation, relative to that of the control sample (S-S). The spectral signature of carbon within the composite matrix is evident in the wavenumber range of 1125-1150 cm^{-1}, as illustrated by the characteristic peaks. Furthermore, the absorption peaks detected at 1500, 980, 1000, and 1100 cm^{-1} across all samples could be linked to either silicon-oxygen (Si-O) or carbon-oxygen (C-O) bonding, which is indicative of the presence of tricalcium silicate (C_3S) and dicalcium silicate (C_2S) or ether linkages. The observed band could be attributed to either a symmetric (C-O) and non-symmetric stretching vibration ring (-C-O-C) or anti-symmetrical Si-O-Si stretching mode, potentially influenced by the presence of alumina, nanographene oxide, and silica-containing minerals within the sandcrete composite, which may induce vibrational coupling or perturbation in the molecular structure (Ngally Sabouang *et al.,* 2014). The spectral peaks intensities observed at 1350 cm^{-1} and 3580 cm^{-1} are indicative of strong chemical bonds, specifically associated with calcite, $CaCO_3$ (C-O bond), and portlandite ($Ca(OH)_2$) (O-H) species, respectively, suggesting a high degree of molecular interaction and cohesion.

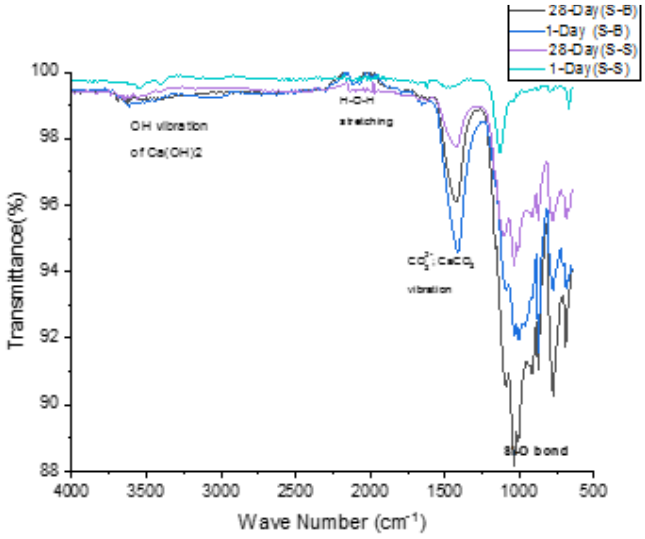

Figure 20: Comparative FTIR analysis of S□S (Control) and S-nGO (B) for 1 and 28 days

4. CONCLUSION

This study investigated the durability, microstructural changes, and the degree of carbonation in sandcrete-nanographene oxide composite using XRD, XRF, TGA, FTIR, EDS, and SEM. The key findings:

1. Early-age carbonation (1–28 days) enhances the durability of the S-nGO composite by refining the microstructure and reducing the porosity, thereby improving the material's overall properties.
2. The incorporation of nGO alters the hydration kinetics of the associated hydrates, exerting a profound influence on the hydration mechanism resulting in decreased porosity after 28 days.

3. Unlike the control without nanographene oxide, the S-nGO matrix composites presented a denser microstructure with a lamellar appearance (foil-like) of a calcium silicate hydrate (C-S-H) phase gel containing more calcium, oxygen, carbon, and silicon.
4. The 0.05% S-nGO composite mixture resulted in the highest carbon dioxide sequestration potential, with a carbonate concentration of 0.0406 kg/m^3, whereas that of the 0% nanographene oxide control sample was approximately 0.0128 kg/m^3 at 30 °C.
5. The findings demonstrated that early-age carbonation (1–28 days) could enhance the durability of the sandcrete–nanographene oxide composite by refining the microstructure and reducing the porosity, thereby improving the material's overall properties and carbon sequestration potential.

5. ACKNOWLEDGMENT

The authors wish to acknowledge the Tertiary Education Trust Fund (TETFund) for providing the following grants: TETF/ES/DR&D-CE/NRF2021/CC/EHU/00045/VOL.1 and TETF/DR&D/POLY/BIDA/IBR/2022/VOL. II/SN 15 for this research.

6. CONFLICT OF INTEREST

There is no conflict of interest associated with this work.

REFERENCES

Abdullahi, M., Odigure, J. O., Kovo, A. S., and Abdulkareem, A. S., (2016). Characterization and Predictive Reaction Model for Cement-Sand-Kaolin Composite for CO_2 Sequestration. *Journal of CO_2 Utilization*, 16, pp. 169–181.

Abdullahi, M., Odigure, J. O., Aliyu, M. B., Aibinu, A. M. and Olarewaju, S. A. (2024). Investigating Calcite-induced Crack Healing Time-dependent Model for Bio-sandcrete using COMSOL Multiphysics Reaction Module. *Journal of the Nigerian Society of Chemical Engineers*, 39(2), pp. 82-99.

Anosike, M. N. and Oyebade, A. A. (2012). Concrete blocks and quality management in Nigeria building industry. *Journal of Enginering Project Production Management,* 2, pp. 37–46.

ASTM (2023). Standard Specification for Concrete Aggregates, (C33-23). American Society for Testing and Materials, West Conshohocken, Pennsylvania: ASTM International.

ASTM (2023). Standard Test Method for Measuring of Rate of Absorption of Water by Hydraulic-Cement Concretes, (C1585/C1585M-13). American Society for Testing and Materials, West Conshohocken, Pennsylvania: ASTM International.

Arya, S. and Seena, P. (2024). Mechanical Properties and Microstructure of Graphene Oxide (GO) Cement Composites: A Review in: Nehdi, M., Hung, M. K., Venkataramana, K., Antony, J., Kavitha, P. E., and Beena, B. R (eds) Proceedings of SECON'23. SECON 2023. Lecture Note in Civil Engineering, Vol 381.Springer, Cham.

Chu, H. Y., Zhang, Y., Wang, F. J., Feng, T. T., Wang, L. G. and Wang, D. N., (2020). Effect of graphene oxide on mechanical properties and durability of ultra-high-performance concrete prepared from recycled sand. *Nanomaterials,*10(9), pp. 1718.

Chang, C.F and Chen, J.W. (2006) The Experiment investigation of Concrete Carbonation Depth. *Cement and Concrete Research*, 36, pp. 1760-1767. http://doi.org/10.1016/j.cemcoures. 2004.07.025.

Cui, H., Yan, X., Tang, L. and Xing, F. (2017). Possible, Pitfall in Sample Preparation for SEM Analysis-Analysis-A Discussion of The Paper 'Fabrication of Polycarboxylate, Graphene Oxide Nanosheet Composites by Copolymerization for Reinforcing and Toughening Cement Composites' By Lv *et al., Cement and Concrete Composites*, 77, pp. 81-5.

Devi, S. C. and Khan, R. A. (2020). Influence of Graphene oxide on Sulfate Attack and Carbonation of Concrete Containing Recycled Concrete Aggregate. *Construction and Building Materials,* 250, pp. 118883.

Fernandez, B. M., Simons, S., Hills, C. and Carey, P. (2004). A review of accelerated carbonation technology in the treatment of cement-based materials and sequestration of CO_2. *Journal of Hazardous Materials,* 112(3), pp. 193–205.

Fonseka, I., Mohotti, D., Wijesooriya, K., Lee, C., and Mendis, P., (2024). Influence of graphene Oxide Properties, Superplasticiser Type, and Dispersion Technique on Mechanical Performance of Graphene Oxide-added Concrete. *Construction and Building Materials*, 428, pp. 136415.

Gajda, J. (2001). Absorption of atmospheric carbon dioxide by Portland cement concrete. *Portland Cement Association Research and Development, 2255a*, 20.

Gambhir, M. L. (2007). *Concrete Technology* (3rd ed). New Delhi: Tata McGraw-Hill Publishing Company Ltd.

Handayani, M., Sulistiyono, E., Rokhmanto, F., Darsono, N., Fransisca, P. L., Erryani, A., and Wardono, J. T., (2019). "Fabrication of Graphene Oxide/Calcium Carbonate/Chitosan Nanocomposite Film with Enhanced Mechanical Properties." *IOP Conference Series: Materials Science and Engineering*, 578, pp. 012073.

Jafarnia, M.S.; Khodadad Saryazdi, M.; Moshtaghioun, S.M. (2020). Use of Bacteria for Repairing Cracks and Improving Properties of Concrete Containing Limestone Powder and Natural Zeolite. *Construction and Building Materials,* 242, pp. 118059.

Liu, C., Chen, F., Wu, Y., Zheng, Z., Yang, J., Yang, B., Yang, J., Hui, D. and Luo, Y. (2021). Research progress on individual effect of graphene oxide in cement-based materials and its synergistic effect with other nanomaterials. *Nanotechnology Reviews*, 10, pp. 1208–1235.

Lv, S. H., Ma, Y. J., Qiu, C.C., sun, T., Liu, J. J. and Zhou, Q. F. (2013). Effect of graphene oxide nanosheets of microstructure and mechanical properties of cement composites. *Construction and Building Materials,* 49, pp. 121-7.

Lv, S.H., Zhang, J., Zhu, L.L and Jia, C.M. (2016). Preparation of Cement Composites with ordered microstructures via doping with graphene oxide nanosheets and an investigation of their strength and durability. *Materials*, 9(11), pp. 924.

Lin, C. Q., Wei, W. and Hu, Y. H. (2016). Catalytic behaviour of graphene oxide for cement hydration Process. *Journal of Physics and Chemistry of Solids*, 89, pp.128-33.

Lima-de-Faria, J. (1994). Nanographene oxide, in Structural Mineralogy-an Introduction. Kluwer: The Netherlands, pp. 227 – 228.

Long, W. J., Gu, Y. C., Xing, F. and Khayat, K. H. (2018). Microstructure development and Mechanism of Hardened Cement Paste Incorporating Graphene Oxide during Carbonation. *Cement and Concrete Composites,* 94, pp.72-84.

Mohammed, A., Sanjayan, J. G., Nazari, A. and Al-Saadi, N. T. K. (2018). The Role of Graphene Oxide in Limited Long-term Carbonation of Cement-based Matrix. *Construction and Building Materials,* 168, pp. 858-66.

Naik, T. R., Kumar, Rakesh, and Kraus, R. N. (2009). Carbon dioxide sequestration in Cementitious products. *CBU-REP-650*, pp. 124.

Naik, T. R. and Kumar, R. (2010). Global warming and cement-based materials. UWM *centre for byproducts utilization*, Milwaukee, Wisconsin, USA, pp. 1 – 70.

Ngally Sabouang, C. J., Mbey, J. A., Liboum, Thomas, F. and Njopwouo, D. (2014). Talc as raw material for cementitious products formulation. *Journal of Asyian Ceramic Societies*, 2(3), pp. 263-267. https://doi.org/10.1016/j.jascer.2014.05.007.

Odeyemi, S. O., Giwa, Z. T. and Abdulwahab, R., (2019). Building Collapse in Nigeria (2009 – 2019), Causes and Remedies- A Review. *Journal of Science and Engineering Production*, 1 (1), pp. 122-135.

Odigure J. O. (2002). Deterioration of long-serving Cement-based Structures in Nigeria. *Cement and Concrete Research,* 32, pp. 1451 – 1455.

Omoregie, A. (2012). Impact of Vibration Time on Compressive Strength of Hardened Sandcrete Building Blocks. *Buildings,* 2, pp. 153-172.

Odigure, J. O. (1994). Hydration of cement paste and concrete from raw mix containing Metallic particles. *Journal of Cement and Concrete Research*, 24 (8), pp. 1549-1557

Odigure, J. O. (1996). Kinetic Modelling of Cement Raw Mix Containing Iron Particles and Clinker Microstructure. *Journal of Cement and Concrete Research*, 26(9), pp. 1435-1442

Oyekan, G. L. and Kaniyo, O. M. (2011). A study on the Engineering Properties of Sandcrete blocks produced with rice husk ash blended Cement. *Journal of Engineering and Technology*, 3(3), pp. 88 – 98.

Rostami, V., Shao, Y., Boyd, A. J. and He, Z. (2012). Microstructure of paste subject to early carbonation curing. *Cement and concrete research,* 42, pp. 186 – 193.

Raina, V. K and Goyal, S. K. (2015). Influence of Silt Content on the Workability and Strength of Concrete. *International Journal of Advance Research in Civil Engineering* (IJARCE), 4(2), pp. 1-8. https//www.

Shah, T. C. (2005). *CO_2 Sequestration in concrete*. Master of Science in Engineering, Thesis, University of Wisconsin-Milwaukee.

Sunho, C., Jeffrey, H. D. and Christopher, W. J. (2009). Adsorbent Materials for Carbon Dioxide Capture from large anthropogenic point sources. *ChemSusChem*, 2, pp. 796 – 854.

Song, J., Wang, X. and Chang, C., (2014). Preparation and Characterization of Graphene Oxide. *Journal of Nanomaterials*, 2014 (2), pp. 1- 6.

The Nigeria Industrial Standard (NIS) (2007). Draft Code of Practice for Sandcrete Blocks, Federal Ministries of Industries, Lagos, Nigeria.

Turcry, Ph., Oksri-Nelfia, L., Younsi, A. and Aït-Mokhtar, A. (2014). Analysis of an Accelerated Carbonation Test with Severe Preconditioning. *Cement and Concrete Research*, 57, pp. 70 – 78.

Varzina, A., Phung, Q. T., Perko, J., Jacques, D., Maes, N. and Cizer, O. (2022). Synergistic Effects between Carbonation and cracks in Hardened Cement Paste. *Sustainability*, 14, pp. 8572. https://doi.org/10.3390/su14148572

Wang, Q., Wang, J., Lu, C. X., Liu, B. W., Zhang, K. and Li, C. Z. (2015). Influence of graphene Oxide additions on the microstructure and Mechanical Strength of cement. *New Carbon Materials*. 30 (4), pp. 349-56.

Younsi, A., Turcry, Ph., Aït-Mokhtar, A., and Staquet, S. (2013). Accelerated Carbonation of Concrete with High Content of Mineral Additions: Effect of Interactions between Hydration and Drying. *Cement and Concrete Research*, 43, pp. 25–33.

Yang, H. B., Monasterio, M., Cui, H. Z. and Han, N. X. (2017). Experimental study of the effects of graphene oxide on microstructure and properties of cement paste composite. *Composites part A-Applied Science and Manufacturing,* 102, pp. 263-72.